II

PHENOMENOLOGICAL INTRODUCTION TO PHOTON HADRON INTERACTIONS

P. SÖDING

DESY
2 Hamburg 52, Allemagne Fédérale

1. Introduction

In these lectures we will discuss how the structures and interactions of hadrons are experimentally investigated by probing them with photons and electrons. It is well known how successfully this works for the elastic form factors of the proton and neutron. The success is due to the fact that the photon is a comparatively simple object. This in turn comes from its relatively weak coupling to other particles, being proportional to the elementary charge $e = \frac{1}{\sqrt{137}}$. This means that one usually needs to consider only the lowest order in e. Further, the purely electromagnetic interaction is well understood (thanks to Maxwell, Dirac and Feynman) and can be calculated, without catastrophic infinities etc. and

Thus, in electron hadron scattering the dominant lowest order process

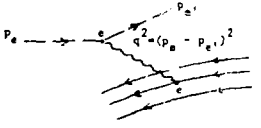

has just one simple object, the photon, interacting with the hadronic electromagnetic current in a single electromagnetic interaction with coupling constant e. By contrast, hadron hadron scattering involves extended multiple interactions of two very complex strongly interacting systems.

In view of the quite special properties of the photon it is remarkable that it can also appear hadron-like. That is, in some of its interactions with hadrons the photon behaves as if $\frac{1}{137}$ of the time it was a hadron itself, showing the same gross features of the interactions, only scaled down in probability by e^2. A photon beam offers then the same experimental possibilities as a hadron beam; it is a neutral hadron beam in disguise with vector quantum numbers ($J^{PC} = 1^{--}$, mixed I^G). It has the additional bonus that we can

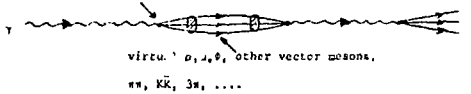

... mass of the pion is ... and, for virtual photons, the mass of the beam particles.

Thus, these scattering features should by photon-hadron interactions ("elementary" and "hadron-like") afford a variety of ways to explore the strong interactions and the hadronic systems existing by the strong interactions.

In these lectures we will concentrate on high energy photon hadron interactions. Still, we will quantum electrodynamics, resonance physics, and e^+e^- interactions, the latter being treated in another lecture. The principal references on the subject matter, which have also been freely used in preparing these lectures, are the summary articles in the Proceedings of the International Symposium on Electron and Photon Interactions at High Energies at Bonn (1973), and Feynman's book on "Photon-hadron Interactions" (1972).

a) Polarized photon beams

Since an important property of photons is that they can be polarized, we start by discussing practical methods of doing so.

(a) Coherent bremsstrahlung from a diamond monocrystal[1]

Ordinary bremsstrahlung beams have at most a few percent of polarization. However, in the bremsstrahlung of high-energy electrons on the atoms of a regular lattice, the atoms can recoil coherently if the momentum transfer to the atom coincides with a vector of the reciprocal lattice, because their wave functions are then superposed all with the same phase (this is the Bragg condition). Since thereby a particular recoil direction is strongly enhanced, the photons in this case turn out to be linearly polarized, with a

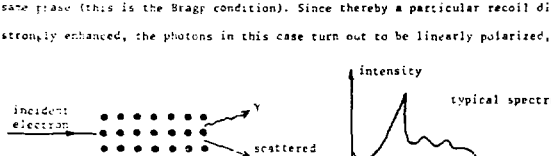

polarization of up to ~70 %. Rather intense beams can be produced. Large polarization is, however, achieved only for $E_\gamma \gtrsim \frac{1}{2} E_{inc}$. Furthermore, there is a flat unpolarized photon background extending up to $E_\gamma^{MAX} = E_{inc}$.

(b) "Acceleration" of polarized light[2]

Light from a laser is Compton-scattered under ~180° on high-energy electrons. The backscattered photons thereby achieve high energy in the laboratory system. As Compton

scattering in the classical (kinematic) region, the final-state photon energy E_γ depends only on the scattering angle, θ. One therefore obtains a nearly monochromatic photon beam by sufficiently collimating the electron and photon beams. The polarization of the laser photons (or, equivalently, of the laser light) is essentially retained in the scattering process, and a high 90 % polarization has been achieved at SLAC. The γ beam is, however, small in intensity and short pulse time duration and is thus essentially limited to experiments in the counting

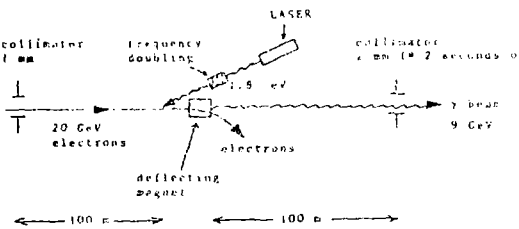

(c) Coherent absorption of photons[3]

When a beam of high energy photons is passed through oriented single crystals of graphite (a 1 mm thick diamond would do also!), one of the linear polarization components is more strongly absorbed than the other, depending on the relative orientation of the polarization vector and the crystal axis. This is due to coherent e^+e^- pair production. By this method also the high energy portion of a bremsstrahlung spectrum can be polarized. One achieves polarizations of ~70 %.

(d) Polarization properties of virtual photon beams[4]

A virtual photon beam, produced by scattering of (unpolarized) electrons, is automatically partially polarized. The effective direction of the polarization (a polar vector) must be in the scattering plane. In contrast to a real photon, however, a virtual photon has both transverse and longitudinal components of its polarization vector. Let us define

$$\varepsilon = \frac{1}{1 + \frac{2(\nu^2 - q^2)}{4EE' - q^2}} = \frac{1}{1 + 2(1 - \frac{\nu^2}{q^2})\tan^2\frac{\theta}{2}} \qquad (1)$$

where the kinematical quantities are q^2 = mass^2 of the virtual photon, ν = its energy,

E(E') the incident (scattered) electron energy and θ the electron scattering angle:

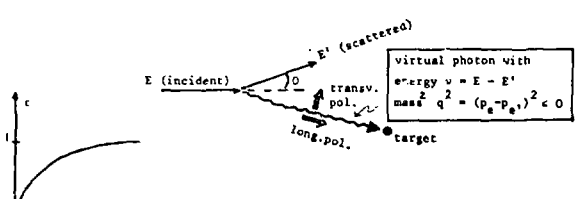

In practice, ε depends mainly on E and E' as shown in the sketch at left.

Then the transverse part of the virtual photon is polarized to degree ε, with the polarization vector of course in the scattering plane; in addition there is a longitudinal polarization component that has total intensity ε times the total intensity in the transverse components, and is coherent with the transverse component in the scattering plane.

In high energy experiments with real photons, one could probably as well use virtual photons of very small q^2 which should behave in a very similar way, but have the advantages of being already polarized and having well-defined energy.

3. Pseudoscalar Meson Photoproduction

Among the simplest reactions of photons with hadrons we have

$$\begin{aligned} \gamma p &\to \pi^+ n \\ \gamma n &\to \pi^- p \\ \gamma p &\to \pi^0 p \\ \gamma p &\to \pi^- \Delta^{++} \\ \gamma p &\to K^+ \Lambda \quad \text{etc.} \end{aligned} \tag{2}$$

Detailed studies of these reactions with incident photons (often polarized) of up to 16 GeV have been made, mainly with large spectrometers measuring only one particle and using the missing mass technique. The basic properties found are as follows. The differential cross sections are falling strongly with increasing energy. They are largest in or near the forward direction; in this general region ($|t| \leq 3$ GeV^2) the approximate s and t dependences are

$$\frac{d\sigma}{dt} \sim s^{-2} e^{3t} . \tag{3}$$

In the forward direction ($\theta = 0$) some of them show a dip, others a spike. There is also a (flatter) backward peak with strong energy dependence,

$$\frac{d\sigma}{dt} \sim s^{-3}. \tag{4}$$

Between the forward and backward regions there is a "central" region ($-t \approx -u \approx s/2$, $\theta \sim 90^{\circ}$) where $\frac{d\sigma}{dt}$ is rather flat and the energy dependence very strong, like s^{-7} or s^{-9}. The behavior is summarized in fig.1 and 2 [5].

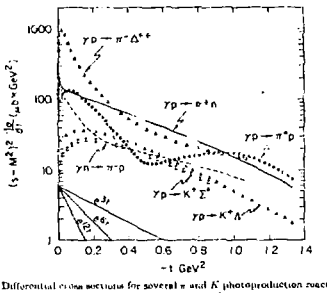

FIG. 1. Differential cross sections for several π and K photoproduction reactions, as a function of four momentum transfer squared. The kinematic quantity $(s - M^2)^2$ is proportional to k^2 (the laboratory photon energy) and is used to make the cross sections essentially independent of energy over the range 3 to 16 GeV.

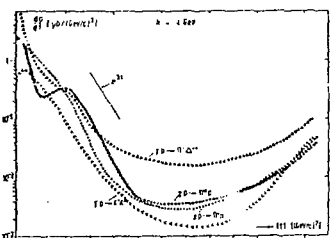

Fig. 2. Combined plot of freehand smooth curves through data for $\pi^+ n$, $\pi^0 p$, $\pi^+ \Delta^{++}$ and $K^+ \Lambda^0$ at 4 GeV incident energy.

The interesting question now is whether or not these photoproduction reactions behave like hadronic reactions. For hadronic two-body exchange processes we have Regge theory, so we will try to apply it here also. What do we know about Regge?

Regge tells us that exchange amplitudes are described by a superposition of Regge trajectories, like

$\pi, \delta;\ \rho, A_2;\ \omega, \ldots,\ K^*, \ldots$ $\quad s \to$ 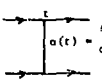 $\quad \alpha(t) =$ angular momentum of the exchange

and that

$$\frac{d\sigma}{dt} \sim s^{2\alpha(t)-2} = \begin{cases} s^{-1} + s^{-2} & \text{(meson exchange)} \\ s^{-3} & \text{(baryon exchange)} \\ s^{-10} & \text{(exotic exchange)} \end{cases} \qquad (5)$$

It is further known from hadronic reactions that absorptive effects (cuts) must also be present:

The s dependence (4) in the backward direction is compatible with our expectation for baryon trajectory exchange. However, from the s^{-2} behavior in the small $|t|$ region one deduces an effective trajectory $\alpha_{eff}(t) = 0$. If this is an asymptotic property it is difficult to reconcile with Regge theory, since we would expect $\alpha_{eff} \sim 0.5$ near $t = 0$ from the ρ, ω and/or A_2 trajectories. Thus we assume at present that it is due to a superposition of several terms of different sizes and s dependences, and that it will change eventually at higher energies.

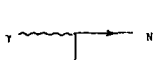

We now discuss the <u>dip/no dip behavior at the very forward angles</u>. Regge theory, as well as any theory of particle exchanges, leads to the following rule:

Let $\Delta\lambda_1$ and $\Delta\lambda_2$ be the helicity change between the in- and outgoing particles at the two vertices, then the

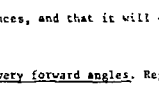

$$\text{amplitude} \sim \begin{cases} \sqrt{-t}^{\,|\Delta\lambda_1| + |\Delta\lambda_2|} & \text{(i.e. dips unless } \Delta\lambda_1 = \Delta\lambda_2 = 0\text{) without absorption} \\ \sqrt{-t}^{\,|\Delta\lambda_1 - \Delta\lambda_2|} & \text{(i.e. dips unless } \Delta\lambda_1 = \Delta\lambda_2\text{)} \quad \text{with absorption} \end{cases} \qquad (6)$$

Explanation of the rule[6]

In the leading eikonal amplitude at high s, the polarization of the exchanged system is coupled to the momenta of the external particles, not to their spins. This leads to the highest powers of the momenta, and therefore of s. E.g. for vector exchange (j = 1),

$$\text{ampl.} \sim \sum_{\text{pol}} (p_1 \cdot e)(p_2 \cdot e) \sim p_1 \cdot p_2 \sim s$$

Consequently, the spin of the exchanged system does not carry any longitudinal component j_z of angular momentum. This holds as well for higher exchanges. Thus, if there is helicity flip of the external particles, i.e. their j_z is changed by $\Delta\lambda$, it must be carried by orbital angular momentum, and thus the amplitude assumes a factor $p_\perp^{|\Delta\lambda|}$ or $\sqrt{-t}^{|\Delta\lambda|}$ for each vertex (the longitudinal momentum $p_{//}$ obviously does not contribute to j_z). However, absorption effects can smear out a zero of the amplitude; the only strict requirement that remains is then a factor $\sim\sqrt{-t}^{|\Delta\lambda_1 - \Delta\lambda_2|}$ which comes from overall angular momentum conservation (the amplitude contains a factor $d^J_{\lambda_i \lambda_f}(\theta) \sim \theta^{|\lambda_i - \lambda_f|} \sim \theta^{|\Delta\lambda_1 - \Delta\lambda_2|}$ for small θ).

Now we compare this rule with the data.

(1) $\gamma N \to \pi^+ N$

We expect $\pi + \rho + A_2$ exchange; since the π pole is so near to $t = 0$, it should dominate there. For π exchange by a nucleon, a simple calculation shows the helicity to flip due to parity. Thus without absorption a forward dip is expected but with absorption this is not necessary, and in fact no dip is observed (Fig.).

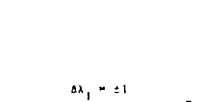

(2) $\gamma N \to \pi\Delta$

This is the same as above except that due to $m_\Delta \neq m_N$ the baryon helicity is not forced by the pion to flip; thus there exists a $\Delta\lambda_2 = 0$ contribution which vanishes in the forward direction due to angular momentum conservation. Thus we expect, and in fact observe, a forward dip (Fig.).

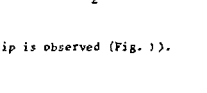

(3) $\gamma N \to \pi^0 N$

π^0 exchange is forbidden by C parity; ω and ρ^0 are possible exchanges and ω should dominate because of its larger coupling ($\Gamma_{\rho\pi\gamma} \ll \Gamma_{\omega\pi\gamma}$). There is nothing to forbid a no-flip amplitude at the nucleon vertex (charge coupling of the ω), thus a forward dip is expected. This again is observed (fig. 1); the superposed very sharp spike in the π^0 cross section at very small $-t$ is due to photon exchange. The shallow minimum at $-t \approx 0.5$ GeV^2 is where the ω trajectory $\alpha_\omega(t)$ goes through zero and the signature factor $1 - e^{-i\pi\alpha(t)}$ in the Regge amplitude vanishes.

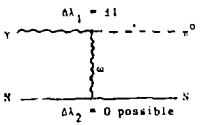

Thus we find reasonable qualitative agreement with our expectations, which are based on our general knowledge of hadronic reactions.

Next we remark on the central region (Fig. 2). This region shows a strong similarity with the corresponding kinematic region in elastic $\pi^\pm p$ scattering; in fact here

$$\frac{d\sigma}{dt}(\gamma p \to \pi^+ n) \approx \frac{1}{217} \cdot \frac{d\sigma/dt(\pi^+ p \to \pi^+ p) + d\sigma/dt(\pi^- p \to \pi^- p)}{2}$$

where $\frac{1}{217}$ is the ratio between $\sigma_{tot}(\gamma p)$ and the average of $\sigma_{tot}(\pi^+ p)$ and $\sigma_{tot}(\pi^- p)$. This shows that at the highest momentum transfers we seem to have a striking agreement between hadronic scattering and photoproduction. Models of hadron compositeness[7] lead to the prediction that in this central region

$$d\sigma/dt(\gamma N \to \pi N) \sim s^{-7}$$
$$d\sigma/dt(\pi N \to \pi N) \sim s^{-8}$$

the pion being composite (in contrast to the photon) causing a faster falloff with energy. Unfortunately the cross sections are getting so small that it will be hard to check this over a wide range of energies.

Measurements with polarized photons

These can give many new types of information. In particular, there is a polarization theorem for photoproduction of pions:[8]

Let $\sigma_\parallel$ and $\sigma_\perp$ be the cross sections for photons with transverse polarization vector parallel and perpendicular, respectively, to the production plane of the pion. Then for high s,

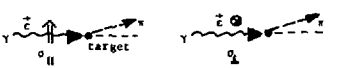

$\sigma_\perp$ gets contributions only from natural parity exchange $(j^P = 0^+, 1^-, \ldots)$

$\sigma_\parallel$ " " " " unnatural " " $(j^P = 0^-, 1^+, \ldots)$

Explanation of the theorem:

First for 0^- exchange (unnatural): reflect on scattering plane (= plane of paper):

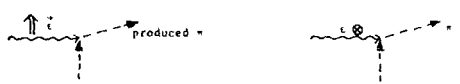

the left picture remains invariant (thus $\sigma_\parallel \neq 0$ allowed) while the right one does not (since the polarization vector ⊗ changes into ⊙ (out of plane)), thus $\sigma_\perp$ must vanish.
Now for 0^+ exchange (natural): the argument is just the opposite since the odd number of pseudoscalar pions present causes an additional change of sign under reflection.
Now for the general case of arbitrary exchanged spin j:

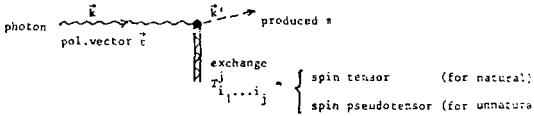

To build a matrix element we can use the vectors $\vec{\varepsilon}$ (once), $\vec{k}$, $\vec{k}'$, and the (pseudo-)tensor $T^j_{i_1 \ldots i_j}$ (which also can occur only once). For the leading term in s, the j polarization vector indices of $T^j_{i_1 \ldots i_j}$ are coupled to $\vec{k}$ and/or $\vec{k}'$, but not to $\vec{\varepsilon}$ or $\vec{n} \propto \vec{k}'$ (which is $\propto k'_\perp$ and therefore small), by the argument given before. Since the total matrix element must be a pseudoscalar because of the pion, if the exchange

is a { pseudotensor (unnatural) we must have no cross product, i.e. a term $\vec{\varepsilon} \cdot \vec{k}'$
tensor (natural) " " " some cross product, i.e. a term $\vec{\varepsilon} \cdot (\vec{k} \times \vec{k}')$.

The measurements with polarized γ of the reaction $\gamma p \to \pi^+ n$ show a polarization asymmetry $\Sigma = \frac{\sigma_\perp - \sigma_\parallel}{\sigma_\perp + \sigma_\parallel}$ as drawn in the sketch. Of course it must be zero in the exact forward direction because there the production plane is undefined. We see that as expected, natural parity exchange (ρ, A_2) dominates at moderate and large $|t|$ values.

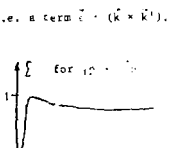

But ... does ... jump from 0 to +1, instead of -1, when we go from $t = 0$ to $|t| = m_\pi^2 = .02$ GeV^2 where we said pion exchange (i.e. unnatural parity) should dominate? There is another related mystery. Fig. 1 shows $\frac{d\sigma}{dt}$ to have a sharp forward spike, although our dip rule only required "no forward dip" and for unabsorbed pion exchange would even require a dip there. On the other hand, the fact that the rapid variation of Σ and $\frac{d\sigma}{dt}$ takes place between $t = 0$ and $-t = m_\pi^2$ definitely suggests that this must have to do with pion exchange.

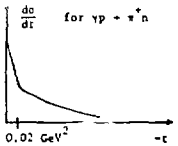

There is a nice explanation of these odd facts. It is connected with the lack of gauge invariance of the pion exchange term. Namely, the $\gamma\pi\pi$ vertex must be a scalar depending on the vectors $\vec{\varepsilon}$, $\vec{k}$ and $\vec{k}'$; furthermore for a real photon $\vec{\varepsilon} \perp \vec{k}$. Thus only $(\vec{\varepsilon} \cdot \vec{k}')$ is possible. But replacement of $\vec{\varepsilon}$ by $\vec{\varepsilon} + \lambda\vec{k}$, i.e. a gauge transformation, gives an additional term $\lambda(\vec{k} \cdot \vec{k}')$ which is in general $\neq 0$. Thus the diagram necessarily violates gauge invariance.

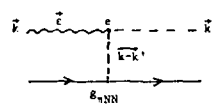

Therefore we cannot take this diagram by itself, but must add other terms to get an invariant overall expression. The pion exchange diagram is proportional to the coupling constants e (electric charge) and $g_{\pi NN}$ (pion nucleon coupling constant); gauge invariance, as a kinematic property, should not depend on the numerical values of these constants. Therefore adding together all possible diagrams that are proportional to $e \cdot g_{\pi NN}$ times kinematical factors, should result in a gauge-invariant expression. These diagrams are

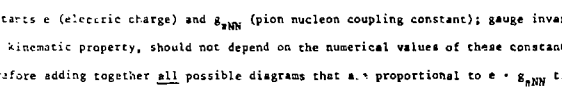

t channel pole — $-\frac{1}{t-m_\pi^2}$

s channel pole — $-\frac{1}{s-m_N^2}$

u channel pole — $-\frac{1}{u-m_N^2}$ (not present for $\gamma p \to \pi^+ n$)

This gauge-invariant sum is called the electric Born term[10] (the full Born term would also contain the couplings of the photon to the anomalous magnetic moments of the nucleon in the s and u channel nucleon exchange diagrams). It is now clear that the pion exchange

term by itself has no precise meaning, but that some nucleon exchange must always be also present. However, the nucleon exchange terms are constant or slowly varying with t such that any rapid variations near $-t = m_\pi^2$ must always be ascribed to the π exchange term.

The electric Born term gives the following amplitudes (again $\parallel$ and $\perp$ refer to $\vec{r}$ being in, or perpendicular to, the production plane):

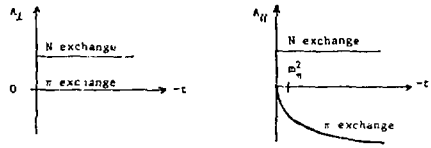

This explains both the forward spike in $\frac{d\sigma}{dt} \propto |A_\perp|^2 + |A_\parallel|^2$ by destructive interference between the N exchange and the rapidly rising π exchange in $A_{\parallel}$, and the asymmetry $\Sigma = +1$ at $-t = m_\pi^2$ where interference is complete.

That pion exchange, made gauge-invariant by adding the other Born terms, can describe the behavior of pion photoproduction at very small $|t|$, although naively from the positive value of the polarization asymmetry Σ one would have guessed quite differently.

For $-t \geq m_\pi^2$ the simple Born term model fails. Here, other exchanges begin to interfere strongly, like ρ and A_2 in the t channel and/or baryon resonances in the s and u channels[11]. The highest trajectories all have natural parity exchange and in accord with this one finds Σ positive and close to 1 for all pion (and kaon) photoproduction processes at $-t \geq 0.5$ GeV^2.

4. Measurement of the pion form factor

This is an application of what we have learned about pion exchange in the previous section, now extended to virtual photons. The diagram is

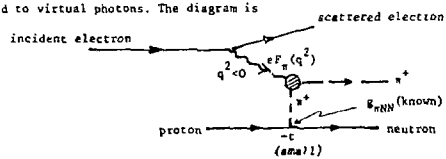

It is clear that we must choose $-t$, the momentum transfer to the nucleon, as small as possible to have a significant contribution of this diagram. The diagram differs from the corresponding one for real photons in the respect that the $\gamma\pi\pi$ vertex is not just proportional to the charge e but contains a numerical factor that describes the q^2 dependence of the photon-pion interaction; this is the form factor $F_\pi(q^2)$ of the pion ($F_\pi(0) = 1$). It is the only unknown quantity in the pion exchange amplitude.

We can also look at this process as an elastic electron-pion scattering process

$$e\pi^+ \to e\pi^+$$

via one-photon exchange, using a target (proton) that contains a bound pion and a neutron which only acts as a spectator.

Of course one also has the other Born terms; however virtual photons, due to their longitudinal polarization (i.e. helicity 0) component, can contribute particularly strongly to pion exchange at small angles as demonstrated below:

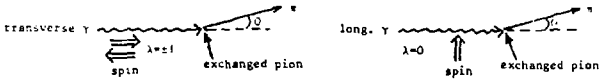

this must vanish for $\theta \to 0$ (ang. mom. cons.) does not vanish for $\theta \to 0$

Thus one measures $\frac{d\sigma}{dt}(ep \to e\pi^+n)$ in the range of small $-t$, for various fixed values of q^2; the result is compared with a calculation of Born terms plus other (hopefully small) contributions, and thus one can determine the factor $F_\pi(q^2)$ multiplying the pion exchange term.

The result[2] is shown in Fig. 3. It is compared there with the simplest model one can make for the pion form factor, namely that it is completely determined by the ρ resonance

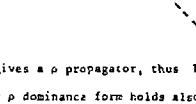

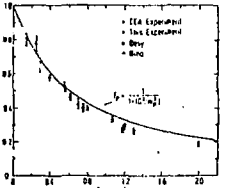

Fig. 3. The π^+ form factor versus Q^2

which gives a ρ propagator, thus $F_\pi(q^2) = \frac{m_\rho^2}{m_\rho^2 - q^2}$ (normalized to 1 at $q^2 = 0$). If this ρ dominance form holds also for large q^2, then for large q^2

$$F_\pi \sim \frac{1}{q^2} ,$$

in contrast to the nucleon form factors which seem to behave more like $\frac{1}{q}$. $F_\pi(q^2) \to 0$ for $|q^2| \to \infty$ of course means that the pion has zero amplitude to appear like a single pointlike object. In the classical picture the charge density is the Fourier transform of $F(q^2)$, thus

$$\rho_\pi(r) = \frac{m_\rho^2}{4\pi} e^{-m_\rho r} \qquad \text{and} \qquad \langle r^2 \rangle_\pi^{1/2} = \sqrt{\frac{6}{m_\rho^2}} = 0.64 \text{ fm}$$

while for the nucleon

$$\rho_N(r) = \frac{a^3}{8\pi} e^{-ar} \quad (a^{-1} = 0.234 \text{ fm}), \quad \langle r^2 \rangle_N^{1/2} = 0.81 \text{ fm}$$

We picture below an intuitive argument why $F_\pi(q^2)$ may indeed fall less steeply for $|q^2| \to \infty$ than $F_N(q^2)$:

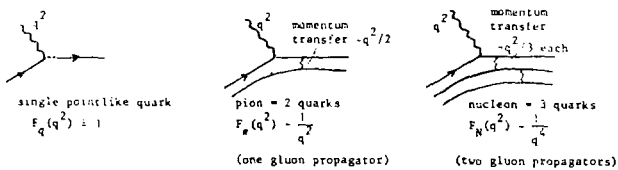

This is of course very naive; however what may be qualitatively right is that the nucleon is more complex than the pion and consequently has less amplitude to hold together under a hard kick (large q^2).

For completeness we consider also the timelike pion form factor. This is measured in e^+e^- annihilation, where at high $s = q^2$,

$$\sigma_{tot}(e^+e^- \to \pi^+\pi^-) = \frac{\pi}{3q^2} e^4 |F_\pi(q^2)|^2$$

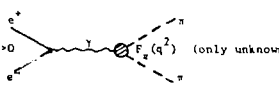

$F_\pi(q^2)$ is complex for $q^2 > 0$; the cross section tells us the magnitude but not the phase. The overall picture is given in the sketch on the next page. Both in the spacelike and timelike regions ρ dominance seems to work rather well. There is no evidence for other large effects, e.g. no additional peaks have been found.

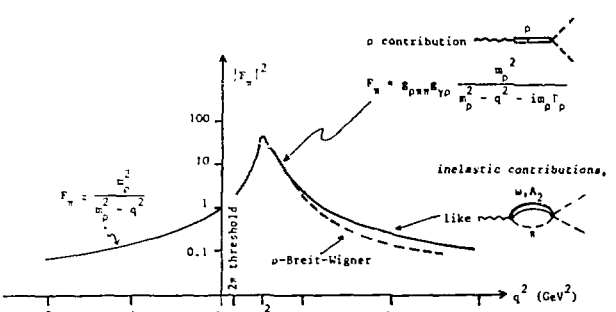

5. Diffraction of photons and ρ^0 photoproduction

It is not really well known what diffraction in high-energy physics precisely is. To explain the general idea we therefore start with the intuitive classical picture.

Consider a plane wave falling onto an absorbing target of radius R. Remember that the scattered wave is always defined as the resulting outgoing wave minus the unperturbed

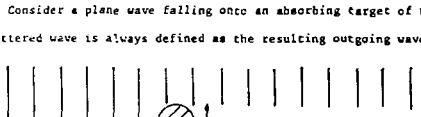

original wave (which would have been present without the absorbing target). Thus the shadow due to the absorption, is produced by an elastically scattered wave interfering destructively with the original wave. This is diffractive shadow scattering, occurring as a necessary consequence of absorption. It leads to a lower bound

$$\left.\frac{d\sigma}{dt}\right|_{t=0} \geq \frac{\sigma_{tot}^2}{16\pi}$$

on the forward elastic differential cross section. In sufficient distance beyond the to get

The wave diffracts into the geometrical shadow region, the angular width of the scattering distribution being a function of the size R of the absorbing object.

From this, the basic properties of diffraction follow:

(i) $d\sigma/dt$ is peaked at small t, the width being $\sim 1/R^2$; the differential cross section is independent (apart perhaps from log s terms) of s.

(ii) The scattering amplitude f(0) (not to be confused with the wave function) is predominantly positive imaginary, this is the condition for destructive interference leading to shadow.

(iii) There is coherence between the incident and the scattered waves, which necessitates identical quantum numbers of the incident and scattered particles.

Elastic scattering of high-energy particles near the forward direction shows these expected diffractive features. Empirically the following additional observations are made:

(iv) *Conservation of s-channel helicity:*

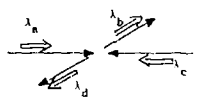

$\lambda_a = \lambda_b$, $\lambda_c = \lambda_d$

(v) There is a wider class of reactions, besides elastic scattering, which show the characteristic properties (i) and, supposedly, (ii). These reactions are different from elastic scattering in the respect that the mass and/or the spin and parity of the incident and scattered particles differ from one another. In these reactions, the exchanged quantum numbers are always those of the vacuum (Pomeron exchange). Further, it appears as if there is a rule that the naturality $(-)^j P$ of each of the scattering particles is conserved in the process ("Gribov-Morrison rule"). In those cases, however, where the spin j changes in the scattering process, *(iv) does* not hold; in fact no simple polarization law has been found for these cases. (Examples: $\pi^- p \to A_1^-$ (1100)p; $K^+ p \to K^*$(1300)p.)

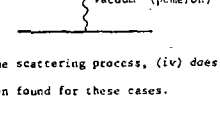

Elastic ("Compton") Scattering of Photons

The reaction process

$$\gamma p \to \gamma p \qquad (7)$$

does show the characteristic features of diffractive scattering in the GeV region, i.e. a nearly s-independent, forward-peaked differential cross section. An example is shown in Fig. 3a.

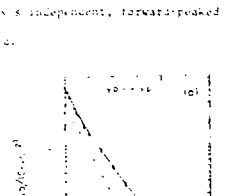

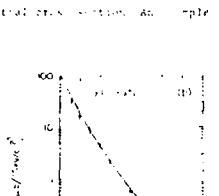

Fig. 3a. Compton scattering at 17 GeV/c (Ref.13)

Fig. 3b. ρ^0 photoproduction at 17 GeV/c (Ref.14)

The size of the Compton cross section is very small,

$$\sigma_{el}(\gamma p) \approx 0.1\ \mu b = \frac{1}{1000}\,\sigma_{tot}(\gamma p),$$

whereas in typical hadronic processes $\sigma_{el} \approx \frac{1}{10}\,\sigma_{tot}$. The explanation is, of course, its proportionality to e^4.

ρ^0 photoproduction[15]

As Fig. 3b shows, ρ^0 photoproduction

$$\gamma p \to \rho^0 p \qquad (8)$$

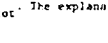

has a very similar shape of $d\sigma/dt$ as Compton scattering and it also is found to be nearly s-independent; however, its cross section is about 200 times larger. We therefore interprete it as diffractive scattering of the virtual ρ^0 component of the photon, the ρ^0 becoming real (on-shell) in the process. This is possible since the γ has a component with

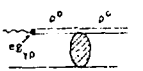

all the conserved quantum numbers identical with those of the ρ^0. The large cross section of reaction (8) as compared with Compton scattering (7) is to be expected since it is a process of first order in the electromagnetic interaction, the cross section being proportional to e^2. We expect, of course, also the process

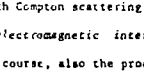

but this is of third order in the e.m. coupling and therefore negligible.

Let us now discuss the properties of diffractive ρ^0 photoproduction in somewhat more detail. The s and t dependences of the differential cross sections are shown for a range of s values in fig. 4; the curves are from a one parameter fit of the relation

$$\frac{d\sigma}{dt}(\gamma p \to \rho^0 p) = e^2 \frac{2}{g_{\gamma\rho}} \frac{d\sigma}{dt}(\rho^0 p \to \rho^0 p) \qquad (9)$$

fitting only $g_{\gamma\rho}$, the photon-rho coupling constant which measures the probability amplitude (in units of e) for a real γ to turn into a virtual ρ^0. The cross section for $\rho^0 p$ elastic scattering is assumed to be equal to the cross section for $\pi^0 p$ elastic scattering

$$\frac{d\sigma}{dt}(\rho^0 p \to \rho^0 p) = \frac{d\sigma}{dt}(\pi^0 p \to \pi^0 p) \qquad (10)$$

as suggested by the simple quark model where the quarks making up the meson scatter on the target independently of whether their spins are parallel (as in the ρ^0) or antiparallel (as in the π^0); isospin zero exchange then gives

$$\frac{d\sigma}{dt}(\pi^0 p \to \pi^0 p) = \frac{1}{2}\left[\frac{d\sigma}{dt}(\pi^+ p \to \pi^+ p) + \frac{d\sigma}{dt}(\pi^- p \to \pi^- p)\right] \qquad (11)$$

Fig. 4 therefore shows that ρ^0 photoproduction has exactly the same s and t dependence as pion-proton elastic scattering, providing additional evidence that it is a diffractive scattering process.

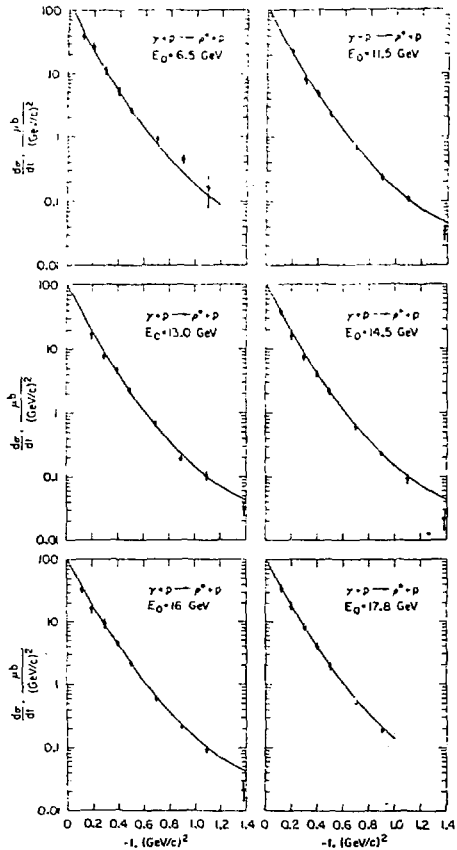

Fig.4. Differential cross section for reaction (8) for different incident photon energies E_0 (ref.16). For the curves, see the text.

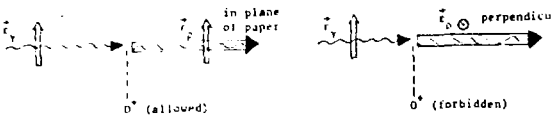

Reflection in the plane of the paper leaves the left picture invariant but not the right one since $\vec{\epsilon}_\rho$ "out" (⊙) changes sign, becoming $\vec{\epsilon}_\rho$ "in" (⊗), thus parity conservation forbids the right hand configuration, i.e. forbids any component of $\vec{\epsilon}_\rho$ perpendicular to $\vec{\epsilon}_\gamma$. If, on the other hand, we exchanged $j^P = 0^-$ instead of 0^+ the result would be just the opposite, since reflection then causes an additional sign change due to the pseudoscalar nature of the exchanged particle; thus in this case any component of $\vec{\epsilon}_\rho$ parallel to $\vec{\epsilon}_\gamma$ would be forbidden. (Eg. in the decay $\pi^0 \to \gamma\gamma$ the polarization planes of the photons must be perpendicular to each other; this in fact is how the intrinsic parity of the π^0 was experimentally determined.) This argument can again be easily generalized to arbitrary exchanged spin in exactly the same way as in the proof of the polarization theorem of section 3. We thus have the parity theorem that

for natural j^P exchange, $\vec{\epsilon}_\gamma$ and $\vec{\epsilon}_\rho$ are parallel to each other
for unnatural j^P exchange, $\vec{\epsilon}_\gamma$ and $\vec{\epsilon}_\rho$ are perpendicular to each other

The polarization vector $\vec{\epsilon}_\rho$ of the ρ^0 is measured by observing the ρ^0 decay in the ρ^0 rest frame, there the decay is characterized by the relative momentum vector $\vec{q}_{\pi^+} - \vec{q}_{\pi^-}$ alone, and thus the only possibility for the matrix element of ρ^0 decay is

$$M = (\vec{q}_{\pi^+} - \vec{q}_{\pi^-}) \cdot \vec{\epsilon}_\rho .$$

Thus if ψ is the azimuthal angle of the relative decay momentum $\vec{q}_{\pi^+} - \vec{q}_{\pi^-}$ measured with respect to the ρ^0 momentum as z axis and $\vec{\epsilon}_\gamma$ as x axis, then the picture is as illustrated here:

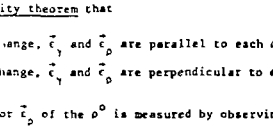

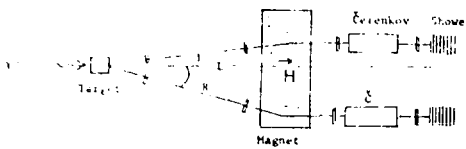

Small counters define the angles ϑ_R and ϑ_L under which the leptons are observed on the right and left side; the magnetic field allows to fix the momenta and the electrons are separated from the background of pions and other particles by Cerenkov and shower conters. First of all, with this arrangement one finds a ρ^0 peak when the effective mass $M_{e^+e^-}$ is in the m_ρ region, which shows that ρ^0's are indeed produced and decay into e^+e^- pairs. To detect the interference term, one now leaves the geometry fixed but changes the sign (up or down) of the magnetic field, this way interchanging the charges of the leptons. The change observed in the counting rate when doing so is proportional to the interference term. In this way one isolates the interference and one finds that, as a function of $M_{e^+e^-}$, it has a relative maximum at $M_{e^+e^-} = m_\rho$. Since there the phase of the ρ^0 Breit-Wigner function is 90°, this demonstrates directly that $T_{\gamma\rho}$ must be predominantly imaginary. A quantitative evaluation of the measurements[17] gives

$$\frac{\mathrm{Re}\, T_{\gamma\rho}}{\mathrm{Im}\, T_{\gamma\rho}}\Big|_{t\,\simeq\,0} = -0.2\ ,$$

a result very similar to what is observed (by measuring the interference with Coulomb scattering) for elastic forward hadron-hadron scattering at similar energies, i.e. in the 10 GeV range.

From all these observed features of ρ^0 photoproduction it is very strongly suggested that indeed it is predominantly diffractive and in fact near the forward direction behaves just like elastic shadow scattering. Thus, the mass change in the scattering from a virtual (mass zero) to a real ρ^0 does not seem to destroy the coherence properties intrinsic in diffractive scattering. Detailed analysis of the measured s and t dependences of the differential cross sections, as well as the helicity structure of the amplitudes, reveals the presence of some non-diffractive scattering also (e.g. from the energy dependence, or unnatural exchange). Thus in order to quantitatively study the properties of the

i.e. if the photon makes a transition into virtual vector mesons, then always into this particular superposition of ρ^0, ω and ϕ.

Note. The Vector-Dominance-Model claims that the photon always interacts with hadrons in a virtual vector meson state, i.e. never "directly" without intervening resonant vector states. This may not be true as is discussed below and in Tran's lecture.

In diffraction production of vector mesons by photons we should expect to produce just the linear combination (15) of ρ^0, ω and ϕ, provided the energy is high enough so that the mass differences are negligible and the elastic scattering amplitudes of the vector mesons on nucleons have the same magnitudes and phases. Thus one would expect to find ρ^0, ω and ϕ in the ratio of 9 : 1 : 2. The experimental values of $\frac{d\sigma}{dt}\Big|_{t=0}$ for ρ^0, ω and ϕ, however, are in the ratio

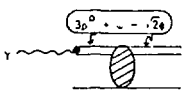

$$110 : 14 : 3 \quad \left(\text{differential cross sections in } \frac{\mu b}{GeV^2}\right)$$

(where for the ω only the diffractive part is taken). This is in violent disagreement with the expectation; the number of ϕ's observed is two small by a factor of 8. A disagreement by something like a factor 2 could presumably be blamed on SU(3) symmetry breaking but a factor 8 certainly can not.

There is, however, a striking explanation for the smallness of ϕ production by the quark model. Assume that in a meson-nucleon collision at high energy the quarks making up the meson scatter independently of each other, such that their total cross sections simply add to give the total meson-nucleon cross section. At high energies p and n quarks should scatter equally (since they belong to the same isospin doublet) while λ quarks may have a different cross section. This model predicts (for energies in the 10 GeV region)

$$\sigma_{tot}(\pi^0 P) = \sigma_{tot}(\rho P) = \sigma_{tot}(\omega P) = \frac{1}{2}\left[\sigma_{tot}(\pi^+ P) + \sigma_{tot}(\pi^- P)\right} = 26 \text{ mb (exp.)}$$
$$\| \qquad\qquad \| \qquad\qquad \| \qquad\qquad \| \qquad\qquad \| \qquad\qquad \| \qquad\qquad \|$$
$$\frac{1}{2}(p\bar{p}-n\bar{n}) \qquad (p\bar{n}) \qquad \frac{1}{2}(p\bar{p}+n\bar{n}) \qquad (p\bar{n}) \qquad (n\bar{p}) \qquad (16)$$

$$\sigma_{tot}(\phi P) = \sigma_{tot}(K^+ P) + \sigma_{tot}(K^- P) - \sigma_{tot}(\pi^- P) = 12 \text{ mb (exp.)}$$
$$\| \qquad\qquad \| \qquad\qquad \| \qquad\qquad \|$$
$$(\lambda\bar{\lambda}) \qquad (p\bar{\lambda}) \qquad (\lambda\bar{p}) \qquad (n\bar{p})$$

i.e. nonstrange quarks (p, n, $\bar{p}$, $\bar{n}$) have total cross sections of 13 mb on nucleons while strange quarks (λ, $\bar{\lambda}$) have only ≈6 mb, resulting in $\sigma_{tot}(\pi N) \approx 26$ mb, $\sigma_{tot}(KN) \approx 20$ mb (one strange quark) and $\sigma_{tot}(\phi N) \approx 12$ mb (two strange quarks). Now $\sigma_{tot}(\phi P)$ smaller by a

The $\rho'(1600)$

In the photoproduction spectrum,

$$\gamma p \to \pi^+\pi^- p,$$

some non-resonant background is found but no other resonances besides the ρ^0 are clearly seen. In the reaction

$$\gamma p \to \pi^+\pi^-\pi^+\pi^- p, \qquad (18)$$

however, the 4π mass spectrum shows an enhancement (called $\rho'(1600)$) at M ~ 1600 MeV with a width Γ ~ 400 MeV (Fig.5). It has

$$\frac{d\sigma}{dt} \propto e^{6t}$$

and a total production cross section of

$$\sigma_{\rho'} \cdot B_{\rho' \to \pi^+\pi^-\pi^+\pi^-} \sim 1.5\ \mu b$$

which appears s-independent from 5 to 16 GeV incident photon energy. As fig. 3 also shows, in its decay the ρ^0 is dominating, thus

$$\rho' \to \rho^0\pi^+\pi^-.$$

The I-spin of the ρ' must be 1, since from the observed $\rho' \to \rho^0\pi^+\pi^-/\rho' \to \rho^0\pi^+\pi^-$ branching ratio of ~0.5 it follows that the ππ system not forming the ρ^0 must have isospin 0.

The J^P quantum numbers of the $\rho'(1600)$ are 1^-; a simplified argument runs as follows:

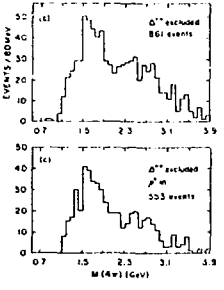

Fig. 5 Four-pion invariant mass distribution from the SLAC streamer chamber experiment on the reaction $\gamma p \to \pi^+\pi^-\pi^+\pi^- p$

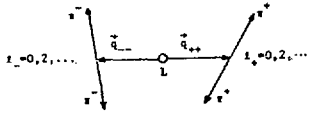

Couple the two π^- together with orbital angular momentum l_-, analogously the π^+ with l_+; call L the orbital angular momentum of the $(\pi^-\pi^-)$ and $(\pi^+\pi^+)$ systems about their common total center-of-mass. Then $\vec{J} = \vec{L} + \vec{l}_+ + \vec{l}_-$. Bose statistics allows only even values of $l_\pm$; since the total mass of the ρ' is not very large, it is reasonable to assume values of $l_\pm = 2$ or higher to be strongly suppressed by centrifugal barriers. Thus $l_\pm = 0$ and $J = L$;

and the $(\pi^+\pi^-)$ and $(\pi^+\pi^+)$ systems each behave like a spin 0 particle. The decay angles is then exactly as for the $\rho \to \pi\pi$, based solely on the relative [illegible]. One finds agreement to all the distributions with the behaviour of the photon [illegible] (as discussed in section 5), i.e. $J^P = 1^-$, helicity conservation and pion [illegible] parity exchange.

All these results strongly suggest that the $\rho'(1600)$ [illegible] diffractively produced by photons. From the observed cross section it is the [illegible] (assuming equal cross sections for ρ' and ρ' elastic scattering) that the coupling probability $f^2_{\gamma\rho'}$ of γ to ρ' is between $\frac{1}{4}$ and $\frac{1}{9}$ of that for the ρ.

Confirmation of the ρ' comes from the Frascati e^+e^- storage ring experiments in which a wide enhancement is found in the reaction

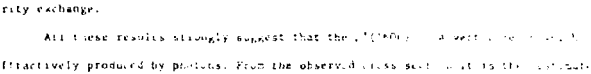

Here it is clear that the state must have $J^P = 1^-$. Thus it is probably due to the same object, the $\rho'(1600)$. However, no clear proof exists that the $\rho'(1600)$ actually is a real resonance; it could e.g. just be a $\rho\sigma$ threshold bump (σ is the s-wave $\pi\pi$ state at 760 MeV), perhaps due to a 4π decay mode of the ordinary $\rho(770)$. Even taking the $\rho'(1600)$, though, eqn.(17) is not yet saturated.

The search for still heavier vector states in diffractive photoproduction has so far been unsuccessful. This does however not necessarily mean that such states do not exist. The problem is that diffractive processes occur at small $|t|$ only, while on the other hand the kinematic minimum of $|t|$,

$$|t|_{MIN} = \left(\frac{m_2^2 - m_1^2}{2E_1^{LAB}}\right)^2 , \qquad (19)$$

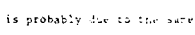

becomes large when the mass m_2 of the produced state becomes large. The formula shows that the only remedy, as for so many other troubles, is higher incident photon energy.

Derivation of the $|t|_{MIN}$ formula (19):
If the energy transferred to the target in the laboratory system is << than the momentum transferred to the target (i.e. minimum momentum transfer << target mass), then

$$\sqrt{|t|_{MIN}} = P_{H1} - P_{H2} = \frac{m_2^2 - m_1^2}{P_{H1} + P_{H2}} \approx \frac{m_2^2 - m_1^2}{2E_1} .$$

The B(1240)

In several photoproduction experiments a bump has been found in the effective mass of the total hadronic system in the reaction

$$\gamma p \to p\pi^+\pi^- \geq 2\pi^0 \qquad (20$$

or

$$\gamma p \to p + \text{missing mass} \qquad (21)$$

at a mass M = 1240 MeV. It is produced with $\frac{d}{dt} \sim e^{5t}$ and a total cross section of ~1 μb, rather energy-independent in the whole observed energy range from 3 to 15 GeV again suggesting a diffractive production mechanism. Since the 2 or more π^0's of reaction (20), were not measured in the experiments (which used bubble or streamer chambers), only their total momentum and energy are known from four-momentum conservation. Thus the decay of the neutral object at 1240 MeV could not be investigated in detail, however it was found that the $\pi^+\pi^-$ mass distribution of reaction (20) in the bump region is consistent with the distribution of the $\pi^+\pi^-$ system from ω decay into $\pi^+\pi^-\pi^0$. This suggests $\omega\pi^0$ decay of the 1240 MeV object; if this is true then $J^{GC} = 1^{+-}$. Two interesting possibilities arise.

(i) The only known resonance which has mass ~1240 MeV and decays into $\omega\pi$, is the B(1240) with $J^P = 1^+$. This is a well-analyzed state[20], copiously produced in the reactions $\pi^+p \to B^+p$. We thus would be observing the reaction

$$\gamma p \to B^0 p \qquad (22)$$

with properties suggesting diffraction. This is interesting because it would violate the empirical "Gribov-Morrison rule" that naturality is conserved in diffractive reactions (see section 5). This rule has no theoretical justification; for example if it is violated it may nevertheless be true that in diffractive processes no quantum numbers are exchanged in the t channel (Pomeron exchange), since there can always be orbital angular momentum between the exchanged and the diffracted particle. The only justification of the rule is a systematics that seems to be apparent in hadronic diffractive and non-diffractive reactions. This systematics may then not hold for photon reactions, or it may not hold in hadronic diffractive reactions either although no exceptions have yet been found there. In any case, for the understanding of diffractive phenomena in general it is important to clear up this question. Here again, higher E_γ will be necessary to verify the energy independence of the cross section, but photon detectors have also to be installed in the experiments in order to measure the individual π^0's and to ascertain whether we are indeed observing the $B \to \omega\pi^0$ with $J^P = 1^+$.

scattering. The same is expected to hold for ϕ photoproduction

$$\gamma P \to \phi P$$

since, analogous to ρ^0 photoproduction, it should just be elastic scattering of the ϕ component of the photon (no quark exchange diagrams can be drawn for $\rho^0 P \to \phi P$ or $\omega P \to \phi P$ either).

Experimentally one finds, as for ρ^0 photoproduction, natural parity exchange and consistence with s-channel helicity conservation; furthermore $\frac{d\sigma}{dt}$ seems rather s-independent (without shrinkage) throughout the whole energy range of observation, from 2 to 19 GeV (Fig.6). Fitting an effective pomeron trajectory using formula (5), one therefore obtains

$$\alpha_{\text{eff}}(0) = 1.0, \qquad \alpha'_{\text{eff}} = 0,$$

i.e. a flat pomeron trajectory. This is to be contrasted with the meson and baryon trajectories which all have slopes of about 1 GeV^{-2}. The ϕ photoproduction result seems compatible with the observations on proton-proton elastic scattering at the CERN-ISR, where at the highest energies a small, perhaps vanishing pomeron slope is found also, with $\alpha'_{\text{eff}} \sim 0.1 \pm 0.2$. It appears then that ϕ photoproduction shows this high-energy (asymptotic?) property already at a much lower energy. One wonders therefore whether ϕ photoproduction at the highest NAL or CERN II energies may not perhaps have surprises for us in store.

7. Diffraction on Nuclei

Interesting physics can also be learnt from studying coherent diffractive vector meson photoproduction on nuclei, e.g.

$$\gamma A \to \rho^0 A. \tag{23}$$

The basic idea is to use nuclei both as production targets and at the same time as absorbing and refracting media of different sizes for the produced vector mesons; this gives information on the ρ^0 nucleon cross section which by other means is hardly measurable, due to the small lifetime ($\sim 10^{-24}$ s) of the ρ.

Consider a photon with momentum $\vec{k}_\gamma$ incident on a heavy nucleus of radius R, producing a ρ^0 of momentum $\vec{k}_\rho$ in a diffractive process on a nucleon at impact parameter b and longitudinal coordinate z. If it is indistinguishable on which of the nucleons the production process has occurred, then the amplitudes for production on the individual nucleons add coherently, all leading to the same final state. In particular, this will be the case

We can then perform the integration over ϕ using the identity

$$\int_0^{2\pi} e^{\pm ix\cos\phi}\, d\phi = 2\pi\, J_0(x)$$

and obtain

$$f(\theta) = f_N(\theta) \int_0^R 2\pi b\,db \int_{-R}^{R} dz\; \rho(b,z)\; J_0(b\Delta_\perp) e^{iz\Delta_\parallel}$$

where we have written the

transverse momentum transfer $\Delta_\perp = k_\rho \sin\theta$

longitudinal " " $\Delta_\parallel = k_\gamma - k_\rho \cos\theta = k_\gamma - k_\rho = k_\gamma - \sqrt{k_\gamma^2 - m_\rho^2}$

$$\simeq \frac{m_\rho^2}{2k_\gamma} = \sqrt{|t|_{MIN}} \qquad (24)$$

(note that because of the large mass of the nucleus, the energy transfer to the nucleus is << than the momentum transfer, thus the energy of the $\rho = k_\gamma$).

Also

$$|t| = \Delta_\parallel^2 + \Delta_\perp^2 \qquad \text{(energy transfer negligible)}$$

thus

$$\Delta_\perp^2 = |t| - |t|_{MIN}. \qquad (25)$$

We see that the angular width of $|f(\theta)|^2 = d\sigma/d\Omega$, or equivalently the width in t of the coherent forward peak, is determined by the Bessel function $J_0(b\sqrt{|t|-|t|_{MIN}})$; for uniform density $\rho(b,z)$ the integration leads to the well known distribution

$$\left[\frac{J_1(R\Delta_\perp)}{\frac{1}{2}R\Delta_\perp}\right]^2 \quad \text{with} \quad \langle |t| - |t|_{MIN}\rangle = \frac{4}{R^2}\,. \qquad (26)$$

The factor $e^{iz\Delta_\parallel}$ expresses the fact that due to energy conservation and $m_\rho > m_\gamma$, the momentum of the ρ^o is $k_\rho = \sqrt{k_\gamma^2 - m_\rho^2} < k_\gamma$ and thus the ρ^o has a longer wavelength. This leads to a condition on longitudinal coherence for an inelastic process: even in the exact forward direction we obviously will have constructive interference of all the single waves only if

$$R \cdot \Delta_\parallel \le 1, \qquad \text{or} \qquad \sqrt{|t|_{MIN}} \le \frac{1}{R}\,. \qquad (27)$$

Thus $|t|_{MIN}^{\sim 1/2}$ is the coherence length. It is 0.8 fm (i.e. nucleon radius) already at the ρ production threshold of $k_\gamma = 1.1$ GeV, and increases proportional to k_γ.

We now consider also the attenuation of th outgoing ρ^o wave by further interactions with the nucleons. Since attenuation of the coherent, nearly forward travelling wave is determined by the total ρ^o nucleon cross section $\sigma_{\rho N}$, a factor

very striking and is an independent, most beautiful confirmation of the quark model concept of scattering discussed in section 6.

8. Shadowing in Nuclei[22]

The total photon-nucleon cross section behaves, as a function of energy, quite similar to hadronic total cross sections; the only difference is its much smaller size. Thus, at high energies it assumes a value of ~120 μb for both protons and neutrons, which is about $\frac{1}{220}$ of the pion-nucleon cross section. It is worthwhile to note that "total photon proton cross section" refers only to the interactions with the proton that are not of purely quantum-electrodynamic type, i.e. to all meson photoproduction processes and their elastic Compton "shadow". QED processes in which the proton takes part only with its Coulomb field are uninteresting in the present context although one of these processes, e^+e^- pair production, has a total cross section on protons of about 21 mb at high energies and accounts essentially for all the attenuation of a photon beam in a target. This means that total photon cross section measurements are not simple attenuation measurements; the hadronic reaction products have to be identified in each interaction.

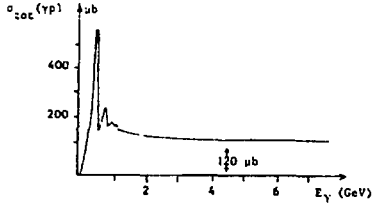

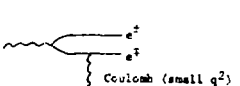

We now discuss photoproduction on nuclei. From the small high-energy photon-nucleon cross section of 120 μb the attenuation length of photons in nuclear matter is expected to be of the order of 500 fm. Thus each nucleon in a nucleus sees the full unabsorbed beam, and one expects a total cross section

$$\sigma_{tot}(\gamma A) \approx 120\ \mu b \times A.$$

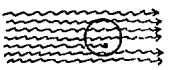

is seen to be the case at high energies, then shadowing is to be expected. The effect should increase with the photon energy ν, until at high ν complete shadowing with $\sigma_{tot}(\gamma A) = A^{2/3}$ is reached.

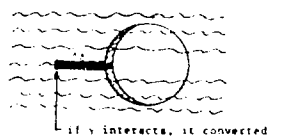

The measured photon shadowing provides therefore direct evidence that the γ does not just interact locally, but that the interaction is spread out over a distance lc which, in our interpretation, is due to the prior transition into a virtual hadron state. The shadowing as observed experimentally in the ν ≈ 15 GeV region is not complete, however; it looks like ~20 % of the interactions is without shadowing (or, perhaps, due to very large hadron masses m_h). If the shadowing increases for real photons with still higher momentum, this would indicate that rather heavy vector states, coupled to the photon, must exist. If it does not, then this may be a hint of a direct, local ("pointlike"), photon interaction perhaps with one of the quarks inside the struck nucleon.

The question may arise here why in our discussion of the reaction $\gamma A \to \rho^0 A$ in section 6, we did not also consider absorption of the photon as, e.g., a virtual ρ^0 state in the nucleus before reaching the interacting nucleon. In fact, we could as well have anticipated the results on photon shadowing there and treated the process from the point of view that the ρ^0 was present already before the nucleus; but then we have to treat the reaction $\rho^0 A \to \rho^0 A$ as elastic shadow scattering. The ρ^0 wave incident on the nucleus is then absorbed away, and this produces a ρ^0 shadow; i.e. a scattered ρ^0 wave appears behind the nucleus which is the difference between the outgoing (absorbed) ρ^0 wave and the original unperturbed ρ^0 wave. The result is the same, according to Babinet's theorem (see e.g. H.Gottfried, Optical Concepts in High Energy Physics, CERN 72-20,p.22).

For virtual spacelike photons ($q^2 < 0$), the arguments given above are expected to be valid also, with the only difference that now $\Delta E = \sqrt{k^2 + m_h^2} - \sqrt{k^2 + q^2} \approx \frac{m_h^2 - q^2}{2k}$ and therefore the characteristic longitudinal spread of the interaction becomes smaller,

$$\langle \Delta r \rangle = \frac{2k}{m_h^2 + |q^2|} \approx \frac{1}{\sqrt{|t|}_{MIN}} \qquad (30)$$

But a new paradox appears: The experiments do not show shadowing, even at rather small values of $-q^2 \approx 0.4$ GeV^2. It seems that the shadowing disappears very rapidly as q^2 becomes $\neq 0$. Do virtual photons perhaps have very different properties from real photons? No reason for this can be seen, as long as $-q^2$ is of the order of or smaller than the squared masses of the hadrons coupling to the photon, i.e. as long as $-q^2 \leq m_\rho^2$. This question has to be further studied experimentally, in particular for higher k and small $-q^2$.

$$\frac{d\sigma}{dq^2 d\nu} = \frac{dN_\gamma}{dq^2 d\nu}\left[\sigma_T(q^2,\nu) + \epsilon\,\sigma_L(q^2,\nu)\right] \tag{33}$$

where $\frac{dN_\gamma}{dq^2 d\nu} = \frac{\alpha^2}{4\pi E^2 m}\left[\frac{2m\nu}{(-q^2)} - 1\right]\left[1 + \frac{4EE' + q^2}{2(\nu^2 - q^2)}\right] = \frac{\alpha^2}{4\pi E^2 m}\left[\frac{2m\nu}{(-q^2)} - 1\right]\frac{1}{1-\epsilon}$

is the number of virtual transverse photons "radiated" by one electron per $q^2\nu$ interval as calculated from Q.E.D..[23] For $q^2 \to 0$, we must have $\sigma_T \to \sigma_{tot}(\gamma P)$ for real photons, and $\sigma_L \to 0$.

There is another equivalent notation which is inspired by analogy with elastic electron proton scattering where

$$\frac{d\sigma}{dq^2} = \frac{d\sigma}{dq^2}\Big|_{point} |F_p(q^2)|^2 .$$

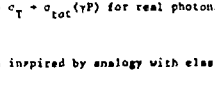

Here, the square of the form factor $|F_p(q^2)|^2$ describes the structure of the scattering hadron, in as much as it differs from a simple point charge. For inelastic scattering one writes correspondingly

$$\frac{d\sigma}{dq^2 d\nu} = \frac{d\sigma}{dq^2}\Big|_{point}\left[W_2(q^2,\nu) + 2(\tan\tfrac{\theta}{2})^2 W_1(q^2,\nu)\right] , \tag{34}$$

thereby defining two "structure functions" $W_1(q^2,\nu)$ and $W_2(q^2,\nu)$ which are analogous to squared form factors. It is clear that there must be two such functions, since they express the non-QED structure of the electron scattering cross section and thus must be in a one-to-one correspondence with the two total cross sections $\sigma_T(q^2,\nu)$ and $\sigma_L(q^2,\nu)$. From a comparison of (33) with (34) one actually finds

$$\begin{aligned} W_1(q^2,\nu) &= \frac{1}{4\pi^2\alpha}\,\nu\left(1 + \frac{q^2}{2m\nu}\right)\sigma_T(q^2,\nu) \\ W_2(q^2,\nu) &= \frac{1}{4\pi^2\alpha}\,\nu\left(1 + \frac{q^2}{2m\nu}\right)\frac{(-q^2)}{\nu^2 - q^2}\left[\sigma_T(q^2,\nu) + \sigma_L(q^2,\nu)\right] . \end{aligned} \tag{35}$$

The QED point cross section

$$\frac{d\sigma}{dq^2}\Big|_{point} = \frac{4\pi\alpha^2}{q^4}\,(\cos\tfrac{\theta}{2})^2\,\frac{E'}{E} \tag{36}$$

in (34) is the differential cross section for elastic scattering of a (spin $\frac{1}{2}$) electron

The total cross sections σ_T and σ_L, or equivalently the structure functions W_1 and W_2, can be determined experimentally as functions of q^2 and ν by measuring $d\sigma/dq^2 d\omega$ for the scattered electron, e.g. in single-arm spectrometers detecting only the electron. It is not trivial to separate σ_T and σ_L or W_1 and W_2; as we see from equ.(33) this must be done varying, at fixed q^2 and ν, the value of ϵ (given by equ.(1)). In order to obtain small values of ϵ, one must make E'/E relatively small thus ϑ large, but under this condition the differential cross section for a fixed solid angle interval of the scattered electron becomes rather small. The separation of σ_T and σ_L is therefore more difficult than the measurement of $\sigma_T + \epsilon\sigma_L$ (where, usually, $\epsilon \sim 1$). For the most recent summary of the experimental results see ref. 24. In accord with our general intention in these lectures, we discuss only the data above the resonance region ($-q^2$ between 0 and 20 GeV^2, $\sqrt{s}$ between 2 and 5 GeV for the SLAC data).

First of all, the general tendency of both σ_1 and σ_L at high energies ν is to fall with increasing $-q^2$, very roughly like $1/q^2$. Thus, virtual photons have smaller cross sections. Further, the ratio $R \equiv \sigma_L/\sigma_T$ is always $\ll 1$; on the average it is ≈ 0.17. The dependence of the total cross sections on ν or s at fixed $-q^2$ is illustrated schematically below:

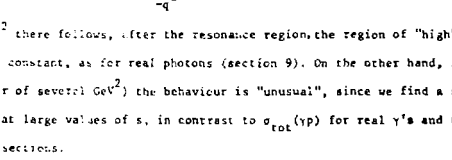

For small $-q^2$ there follows, after the resonance region, the region of "high" energies where σ_T is nearly constant, as for real photons (section 9). On the other hand, for large $-q^2$ (of the order of several GeV^2) the behaviour is "unusual", since we find a strong increase with s even at large values of s, in contrast to $\sigma_{tot}(\gamma p)$ for real γ's and to all hadronic total cross sections.

These experimental results can be better summarized in terms of the structure functions W_1 and W_2. One finds that in the "deep inelastic region", which is defined as the region

$$-q^2 \geq 1 \text{ GeV}^2, \qquad \sqrt{s} \geq 2 \text{ GeV},$$

the quantities $2mW_1$ and νW_2 do not depend significantly on the two variables q^2 and ν separately, but only on their ratio (39), i.e. on the variable $\omega = 1/x = 2m\nu/(-q^2)$. Thus these

expressions are dimensionless functions of ν or x. As shown in Fig. 7. This fact is called "scale invariance", and ν or x is a "scaling variable", for the following reason. We can write (40) in the form

$$\underbrace{\frac{d\sigma}{dq^2\,d\nu}}_{\text{relative } \nu \text{ interval (cross section)}} = \underbrace{\frac{d\sigma}{dq^2}\Big|_{\text{point}}}_{\text{function of only}} \cdot \Big[\underbrace{\tan^2\tfrac{\theta}{2} - \frac{q^2}{2M\nu}\tan^2\tfrac{\theta}{2}}_{\text{kinematic factor for spin 1/2, see (37)}} + \underbrace{\frac{1}{M\nu}\, 2MW_1(q^2,\nu)}_{\text{function of } \nu \text{ only}} \Big] \qquad (40)$$

(...) that the dimensionless quantities νW_2 and $2MW_1$ are functions only of the dimensionless ... quantity ν. Bjorken that the right hand side of this equation does not ... a fixed absolute mass or length scale; it only depends on the pointlike cross sect... and on certain ratios of kinematic variables. This situation is to be contrasted for example with elastic ep scattering, where the elastic form factor contains a fixed length parameter, the mean square radius of the proton; or with diffraction scattering which gives peaks of (more or less) fixed width in t, thus again containing an energy or size parameter, in this case the effective size of the interaction. The absence of such fixed parameters in the cross section for inelastic eP scattering, i.e. the independence of any length scale, suggests that the target in effect acts as if it had no size. We will discuss the parton picture in the next section in order to demonstrate which conclusions one can draw about the structure of the target from the scaling property. It is also interesting that νW_2 is of relatively large absolute size, its maximum being about 0.35; according to formula (40) this means that even at high $-q^2$ the cross section is of the same order of magnitude as for a point charge, quite in contrast with e.g. elastic ep scattering with its strongly vanishing form factor.

The latest inelastic electron scattering results from SLAC indicate deviations from exact scaling[26]; for example νW_2 is found to fall somewhat when ω is held fixed in the region between 1.5 and 3 and $-q^2$ increases from 2 to 15 GeV^2 (fig. 8). Also, results[27] from FNAL on inelastic muon scattering at 150 GeV suggest that νW_2 at large ν and $-q^2$ (small ω) is perhaps 20 % smaller than predicted by scaling the data from lower ν and $-q^2$. These results have still to be confirmed further.

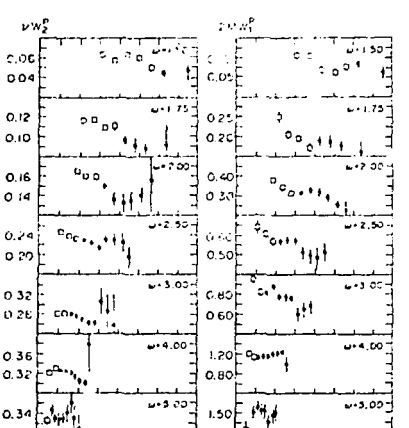

Fig. 8. Proton structure functions versus $Q^2 = -q^2$ for fixed ω (Ref. 20). Note that the scales have suppressed zeros.

10. Partons

In order to better understand intuitively what one learns from inelastic electron scattering, we again compare it with elastic eP scattering.

In elastic eP → eP, one finds a strongly falling form factor $F_p(q^2)$. The proton scatters like a diffuse composite system, comparable to a nucleus as discussed in section 8. If there are constituents, they all scatter coherently since the quantum state of the target hadron remains unchanged and we thus cannot say on which of the constituents the electron was scattered. Therefore, the scattering distribution reveals only the overall spatial distribution of the scatterers, time-averaged because many scattering events are averaged over in one experiment. Scattering into large angles or with large $-q^2$ is strongly suppressed because the coherent addition of the amplitudes cancels it out (Huygens' principle).

On the other hand, in inelastic scattering eP → e + anything the scattering on the individual constituents (if they exist) will be incoherent if the energy transfer is so large that the struck particle is "marked" by its large recoil energy. This of course destroys the coherence. The target hadron "breaks up". The observed scattering distribution can then reveal only the properties of the individual scattering particles ("partons") but does not depend at all on their spatial arrangement, and therefore also scattering under large angles or large $-q^2$ can occur without the destructive interference from the other particles.

Imagine now that the proton indeed has pointlike (or at least very small) constituents (partons).[28,29] The number of virtual partons in a nucleon is of course not fixed but fluctuates since due to the strong binding forces partons can be virtually created and annihilated. In this respect they are analogous to the virtual photons in the field of an electron.

Let us consider an inelastic eP collision at very high momentum ($p \to \infty$) in the cms.

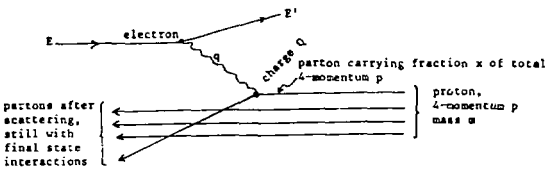

The transverse momenta of the partons before the collision can then be neglected relative to their longitudinal momenta. Call x the fraction of longitudinal momentum = fraction of total four-momentum of the proton, carried by a particular parton (assuming the partons have finite rest mass). Assume that the scattering electron transfers a very hard kick and sufficient energy so that incoherence results. We can then apply the impulse approximation, i.e. assume the scattering takes place on an individual point parton that behaves as if it was momentarily free during the time of interaction with the electron. This is justified due to our assumption of very high momentum p which means the relative motions and the time between interactions among the virtual partons are slowed down by the γ factor; therefore they behave like long-lived non-interacting particles while the electron scatters on one of them.

Comparison with (40) shows that in the parton model

$$\nu W_2 = \sum_i Q_i^2 \, x p_i(x) \qquad \text{(for spin 0 or } \tfrac{1}{2} \text{ of the partons)}$$

$$2MW_1 = \sum_i Q_i^2 \, p_i(x) \qquad \text{(for spin } \tfrac{1}{2} \text{ partons only, } = 0 \text{ for spin 0 partons)} \tag{42}$$

Thus $2MW_1$ and $\frac{\nu W_2}{x}$ as a function of $x = \frac{1}{\omega}$ directly gives us $\overline{Q^2}$ of the partons times the distribution of fractional longitudinal momentum x of the partons, while νW_2 is $\overline{Q^2}$ times the contribution of partons of fractional momentum x to the total momentum. From the apparent proportionality of $2MW_1$ with $\omega = \frac{1}{x}$ at large ω (small x) (fig.7) we see that the number of partons with small fractional momentum x is large $\sim dx/x$; this had already been anticipated by Feynman in order to explain the characteristic properties (e.g. slowly varying high energy total cross sections) of hadron-hadron interactions in the parton picture[28].

From (42) it follows that (Callan-Gross sum rule)

$$\int_0^1 \nu W_2 \, dx = \int_1^\infty \nu W_2 \frac{d\omega}{\omega^2} = \sum_i Q_i^2 \underbrace{\int x \, p_i(x) dx}_{\substack{\text{fraction of proton's total momentum} \\ \text{carried by the i-th parton}}}$$

$$= \overline{Q_i^2} \quad \text{of the partons,}$$

taking a weighted average proportional to the momenta of the partons. Experiment gives 0.18 for protons and 0.12 for neutrons. It follows that if all partons are charged their average charge must be rather small; e.g. if they are quarks, few p quarks but many n or λ quarks must be present. A better assumption is perhaps that there are also neutral particles ("gluons") by the exchange of which the quarks are "glued" together in a hadron state.

Eqn.(42) also shows that if the partons are really pointlike then scale invariance should hold exactly at high energies. The recently suggested violations of scaling can of course be interpreted as being due to a finite size of partons, i.e. to parton form factors. In analogy to the proton form factor $F_p(q^2)$ it may be caused by an interaction of the virtual photon via an unknown neutral vector particle (e.g. a "gluon"). A factor

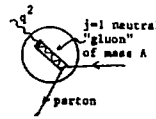

higher and higher energies, then virtual photons in this ω region clearly behave completely different from any known hadrons, as was already pointed out in section 10. This is now seen to be connected with the small value of νW_2 for small ω (or $x \geq 0.7$), i.e. with scattering from the "hard" partons (with large fractional momentum x) of which there are only a few.

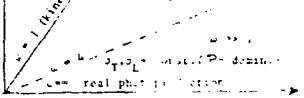

In the deep inelastic region (high $-q^2$ and ν)

for $\omega \leq 4$, $\sigma_T^{\gamma N} = \frac{2\pi\alpha}{\nu} \cdot \left(\frac{\omega}{\omega - q^2}\right)^2 \cdot \frac{1}{(-q^2)}$

for $\omega \gg 4$, $\sigma_T^{\gamma N} = \frac{4\pi\alpha}{(-q^2)}$

(q^2 in $(GeV/c)^2$).

Another indication of peculiar, non-hadronlike high energy behaviour in the domain of small ω is seen in the ratio of νW_2 for neutrons and protons (fig.9). At high energy all hadronic cross sections become equal ($\omega \to 1$ = Pomeron dominance $\Rightarrow I = 0$ exchange) and thus equal on proton and neutron targets; but νW_2 shows, in particular at small ω (large x'), a very strong isospin dependence which persists to the highest energies.

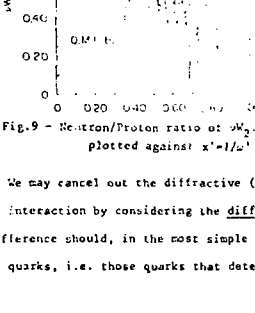

Fig.9 - Neutron/Proton ratio of νW_2.

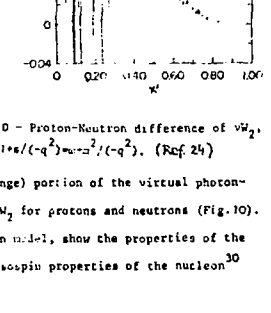

Fig. 10 - Proton-Neutron difference of νW_2, plotted against $x' = 1/\omega'$ where $\omega' = \omega + M_N/(-q^2) = \nu/(-q^2)$. (Ref 24)

We may cancel out the diffractive ($I = 0$ exchange) portion of the virtual photon-nucleon interaction by considering the <u>difference</u> of νW_2 for protons and neutrons (Fig.10). This difference should, in the most simple quark-parton model, show the properties of the valence quarks, i.e. those quarks that determine the isospin properties of the nucleon[30]

11. Hadronic processes by highly virtual photons

We have up to now left out discussion of the final hadronic states created in deep inelastic electroproduction. If the parton ideas are correct - then why do the partons or quarks not come out? This is, together with the too large cross sections observed in e^+e^- annihilation into hadrons (see Renard's lecture), the major theoretical problem with the parton idea.

Even though free quarks are not seen, we can look at the final hadronic states created in deep inelastic scattering to gain insight into the physics underlying the phenomenon of (approximate?) scaling, be it due to quarklike substructures or not. Thus, what are the new features that appear as one goes from photoproduction which as we discussed is "hadronic" in nature, to reactions induced by photons of very high $-q^2$? For example, pointlike substructures could show up through production of hadrons with high $p_\perp$. Or, the "leading" hadrons ejected in the direction of the momentum transferred by the highly virtual photon, could be related to fragmentation of the parton that absorbed this momentum.

The experiments on virtual photon-nucleon interactions are difficult because the cross sections are small (about another factor α^2 compared with photoproduction, see eqn. (69)) and electromagnetic background and radiative corrections have to be dealt with. For certain exclusive 2-hadron final states, counter coincidence or spark chamber experiments have been done in which the electron plus usually one of the hadrons are measured. Similar arrangements are used to measure the single inclusive π, K and P distributions for fixed q^2 and E' of the scattered electron. To measure hadron multiplicities and for unbiased investigations of the gross properties, as well as for exclusive final states, triggered bubble chambers and streamer chambers have been used.

Until now the experiments on particle production by inelastic electron scattering have mainly shown the typical features of hadronic processes, with a few cases however where possibly significant new trends appear. An example of the former type is the pion exchange investigation from which one obtains the pion form factor (as discussed in section 4). Another example is the multiplicity of the charged hadrons.[32] It is found to increase like ln s with coefficient 1, very much like in hadronic reactions:

$$\langle n_{ch} \rangle = \begin{cases} 0.90 + \ln s & (q^2 = 0, \text{ photoproduction}) \\ 0.66 + \ln s & (0.3 < -q^2 < 3\ \text{GeV}^2, \text{ electroproduction}) \end{cases}$$

diffraction we have the longitudinal coherence condition (eqns. (27) and (19)) in the laboratory system

$$\left(\frac{1}{\ell_c}\right)_{MIN} = \frac{m_\rho^2 - q^2}{2\nu} = \frac{m_\rho^2}{2\nu} + \frac{(-q^2)}{2\nu} = \sqrt{|t|_{MIN}}\Big|_{real\,\gamma} + \frac{m}{\omega} \approx \frac{m}{\omega} \leq \frac{1}{R_p}$$

where R_p is the target radius. We can also say: Assuming the γ turns into hadronic states first and these are dominated by the ρ^0 (a very reasonable assumption for diffractive ρ^0 production), then the average distance in the lab travelled by the virtual ρ^0 of mass $q^2<0$ (see eqn. 30) must be

$$\langle \Delta z \rangle = \frac{2\nu}{m_\rho^2 - q^2} = \frac{\omega}{m} \geq R_p \approx 1\ \text{fm} \quad \Longrightarrow \omega \geq 4 \tag{46}$$

for diffraction to take place. If this is fulfilled, the diffractive ρ^0 amplitude will be proportional to

$$e g_{\gamma\rho} \frac{m_\rho^2}{m_\rho^2 - q^2} \tag{47}$$

which is determined by the ρ propagator (remember $g_{\gamma\rho}$ was defined at $q^2 = 0$). Thus we expect the ρ^0 production cross section to be

$$\sigma_\rho(q^2) = \sigma_\rho(q^2 = 0)\left(\frac{m_\rho^2}{m_\rho^2 - q^2}\right)^2 . \tag{48}$$

Fig. 11 shows that indeed the observed σ_ρ (sum of transverse and longitudinal cross sections) behaves roughly as expected for ρ dominance (solid curve).

Note that the total cross section for virtual photons on protons is obviously not dominated by the ρ, since it decreases more like $\frac{1}{q^2}$ rather than like the square of the ρ propagator (47). Thus, the "elastic"/total ratio

$$\frac{\sigma(\gamma_v P \to \rho^0 P)}{\sigma_{tot}(\gamma_v P)}$$

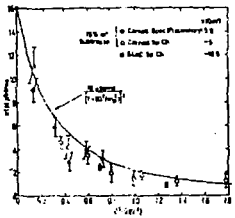

Fig. 11 ρ^0 electroproduction total cross-sections, $\sigma_\rho(Q^2)$, at high energies. ($\nu > 4$ GeV). Ref. 112).

decreases from 13 % at $q^2 = 0$ (a "hadronlike" value) to ~3 % at $-q^2 = 3$ GeV^2. This does

origin (i.e. a $(\omega')^2_{MIN}$ effect) or due only to the switching on of the longitudinal photons or to the decreasing ρ^0 contribution, and that the effect gets more pronounced when $-q^2$ increases more.

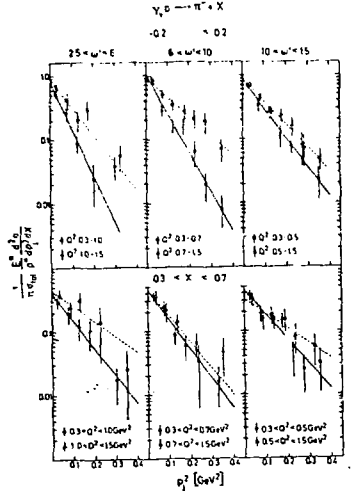

Fig. 3. Distribution of the π^- invariant cross-section over $p_\perp^2$ for different ranges of ω' and x, where $x = p_B^*/p_{MAX}^*$ of the pion in the $\gamma_v P$ cms. Refs. 32, 33.

From what we have discussed it seems probable that at high energies ν, the variable $\omega = \frac{1}{x} = \frac{2\nu}{(-q^2)} + 1 + \frac{s}{(-q^2)}$ is essential in determining whether a photon-hadron interaction is predominantly "hadronlike" or not. Thus for $\omega \gg 4$, including $\omega = \infty$ (real photons), various hadronic states of the photon can appear well before the interaction with the target takes place (eqn. 46); accordingly the hadronic features of the incident photon dominate. In the parton picture, the parton which is hit carries only a small fraction x of the total momentum of the target nucleon; this does not disturb the nucleon much. High energy hadron-hadron interactions are also predominantly involving only these low-x ("wee" x) partons, according to Feynman's parton model.[3,34]

π^+, p^+, ... (= $p\bar{n}$): probability = $(\frac{2}{3})^2 \times 2 = 8$

π^-, $\bar{c}^-$, ... (= $n\bar{p}$): $(\frac{1}{3})^2 \times 1 = 1$

K^+, K^{*+}, ... (= $p\bar{\Lambda}$): $(\frac{2}{3})^2 \times 2 = 8$

K^-, K^{*-}, ... (= ψ): $(= \frac{1}{3})^2 \times 0 = 0$

etc.

The resulting ratios for leading $\pi^\pm$ and $K^\pm$ depend on the unknown fraction of these mesons which come from decays of primarily produced resonances like ρ, K^*, A_2, ... Nevertheless a qualitative tendency of the data to show *increasing* π^-/π^+ *and* K^+/π^+ *ratios for fast forward going mesons when* $-q^2$ increases or ω decreases (i.e. when the picture discussed above becomes applicable), is expected and indeed observed (fig. 14). Note that for a photon behaving hadronlike one expects about equal numbers of leading π^+ and π^- as fragmentation products of the neutral photon (see equn. 15); this is in accord with experiment for $q^2 = 0$ (photoproduction). Thus the observed charge asymmetry at small ω, which can be explained by the direct interaction of the photon with the charge of large-x quarks in the nucleon, could be a striking dynamical manifestation of the unequal charges of the p and n quarks. Of course at present energies ($\sqrt{s} \leq 5$) the leading particles have considerable overlap with other fragments but it will be extremely interesting to follow these and similar other quark features to higher energies in the future. (*A great many interesting ideas in this connection are discussed in Feynman's book.*)

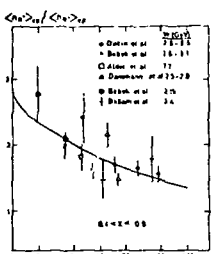

Fig.14. Charge ratio for scattering on a proton target for different measurements. The curve corresponds to a quark parton model fit by Dakin and Feldman (36). In this figure, $x = p_{\parallel}^{\pi} / p_{MAX}^{\pi}$ of the pions in the γ,P cms.

References

1. G. Diambrini-Palazzi, Rev. Mod. Phys. 40, 611 (1968); U. Timm, Fortschr.d.Physik 17, 765 (1969)
2. C.K. Sinclair et al., IEEE Trans. on Nucl. Sci. 16, 1065 (1969)
3. C. Berger et al., Phys. Rev. Letters 25, 1366 (1970)
4. J.W. Akerlof et al., Phys. Rev. 163, 1482 (1967); N. Dombey, Rev. Mod. Phys. 41, 236 (1969)
5. H. Diebold, Comm. Nucl. and Particle Physics 3, 170 (1969); T. Tauman, Proc. Int. Sympos. on El. and Photon Interactions, Bonn (1973) p.145
6. Cf. R.P. Feynmann, Photon-Hadron Interactions, p. 62
7. Cf. F. Salin's review in the Proc. of the Bonn Symposium (1973), p. 261
8. P. Stichel, Zeitschr. f. Physik 180, 170 (1964); J.P. Ader et al., Nuovo Cimento 56A, 952 (1968)
9. For the technique of using 3-space tensors in matrix elements, see C. Zemach, Phys. Rev. 140, B97 (1965)
10. For an explicite demonstration of gauge invariance of the Born term, see Feynman's book, p. 38
11. For example, see I. Barbour et al., Phys. Rev. D4, 1521 (1971); R. Worden, Nucl. Phys. B37, 253 (1972)
12. See R. Talman's review in the Proc. of the Bonn Symposium (1973), p.145
13. A.M. Boyarski et al., Phys. Rev. Letters 26, 1600 (1971)
14. R.L. Anderson et al., Phys. Rev. Letters 25, 1218 (1970)
15. See K. Moffeit's review in the Proc. of the Bonn Symposium (1973), p. 313; and also A.H. Rosenfeld and P. Söding, in Vol. 9 of the Prof. of the International School of Subnuclear Physics, Erice 1971, p. 883
16. R.L. Anderson et al., Phys. Rev. D1, 27 (1970)
17. H. Alvensleben et al., Phys. Rev. Letters 25, 1377 (1970); E. Gabathuler, Experimental Meson Spectroscopy (Ed. Baltay and Rosenfeld), 1970, p. 645
18. The reason is that from the condition on the pion form factor, $F_\pi(0) = 1$, we have for ρ dominance of the form factor the condition $g_{\gamma\rho}g_{\rho\pi\pi} = 1$ (see section 4). Now $g_{\rho\pi\pi}$ is connected with the ρ width by $\Gamma_{\rho\pi\pi} = (g^2_{\rho\pi\pi}/4\pi) \times (m_\rho^2 - 4m_\pi^2)^{3/2} / (3m_\rho^2)$ from which $g^2_{\rho\pi\pi}/4\pi = 2.6$ follows. We therefore see from $g^{-2}_{\gamma\rho}/4\pi = 2.6$ that the ρ dominance

condition is indeed fulfilled.

19. The coupling constants $g_{\gamma V}$ are taken either from the $e^+e^- \to \gamma \to V^0$ measurements at the Orsay storage ring, or from V^0 photoproduction and the quark model as we have described for the case of the ρ^0.

20. See the references quoted in the Review of Particle Properties, Phys. Letters 50B, 1 (1974)

21. For a more detailed discussion and references, see ref. 15.

22. Cf. E. Gabathuler's review in the Proc. of the Bonn Symposium (1973), p. 299

23. To be precise, the number of virtual photons is not unambiguously defined, and neither is the cross section for a virtual particle; only their product is. One can only start from the definition of a real photon cross section and the flux of real photons, and make a reasonable extrapolation of these concepts to off-shell photons. This is what has been done in (33); however other definitions which are equal in the $q^2 \to 0$ limit but differ by kinematic factors for $q^2 < 0$, are also possible. See S.D. Drell and J.D. Walecka, Ann. Phys. 28, 18 (1964); L.N. Hand, Phys. Rev. 129, 1834 (1963); F.J. Gilman, Phys. Rev. 167, 1365 (1968)

24. E.D. Bloom, summary article in the Proc. of the Bonn Symposium (1973), p. 227

25. G. Miller et al., Phys. Rev. D5, 528 (1972)

26. A. Bodek et al., preprint SLAC-PUB-1442 (1974)

27. D.J. Fox et al., preprint CLNS-278 (1974)

28. R.P. Feynman, in High Energy Collisions (Stony Brook Conf.), 1969, p. 237; Phys. Rev. Letters 23, 1415 (1969)

29. J.D. Bjorken and E.A. Paschos, Phys. Rev. 185, 1975 (1969)

30. J. Kuti and V.F. Weisskopf, Phys. Rev. D4, 3418 (1971)

31. D.O. Caldwell et al., Phys. Rev. Letters 33, 868 (1974)

32. See F. Brasse's review in the Proc. of the Bonn Symposium (1973), p. 251

33. V. Eckardt et al., Nucl. Phys. B55, 45 (1973)

34. Cf. also S.M. Berman et al., Phys. Rev. D4, 3388 (1971)

35. C.H. Llewellyn Smith, Phys. Reports 3C, 264 (1972)

36. J.T. Dakin and G.J. Feldman, Phys. Rev. D8, 2862 (1973);
J.T. Dakin et al., SLAC-PUB-1421 (1974)